Human Finger Kinematics and Dynamics

Fai Chen Chen, Silvia Appendino, Alessandro Battezzato, Alain Favetto, Mehdi Mousavi, and Francesco Pescarmona

Center for Space Human Robotics@PoliTo, Istituto Italiano di Tecnologia, Corso Trento 21, 10129 Torino

Abstract. In the last years, the number of projects studying the human hand from the robotic point of view has increased rapidly, due to the growing interest in academic and industrial applications. Nevertheless, the complexity of the human hand, given its large number of degrees of freedom (DoF) within a significantly reduced space requires an exhaustive analysis, before proposing any applications. The aim of this paper is to provide a complete summary of the kinematic and dynamic characteristics of the human finger as a preliminary step towards the development of hand devices such as prosthetic/robotic hands and exoskeletons imitating the human hand shape and functionality. Kinematics and dynamics are presented for a generic finger; with anthropometric data and the dynamics equations, simulations were performed to understand its behavior.

Keywords: Human finger, Kinematics, Dynamics, Extravehicular Activity.

1 Introduction

The human hand is a complex mechanism; it has a wide range of DoFs, allowing a great variety of movements. In recent years, as robotics has advanced, significant efforts have been devoted to the development of hand-related devices. The two main application fields are prosthetic/robotic hands and exoskeletons. On one side, robotic hands are designed to mimic the human hand characteristics, taking advantage of its variety of movements, thereby avoiding the use of a large number of end-effectors when performing tasks with different objects (e.g. Eurobot [1] and Robonaut [2]). On the other side, exoskeletons are designed to fit onto the human hand, aiming at enhancing performance in the carrying out of daily activities (e.g. improving astronauts' hand performance during Extravehicular Activity [3]) or supporting the rehabilitation stage of hand injury recovery.

There are currently many different projects underway. Schabowsky et al. [4] introduced a newly developed Hand Exoskeleton Rehabilitation Robot (HEXORR); which was designed to provide a full range of motion for all fingers. NASA and General Motors presented a prototype of the Human Grasp Assist device [5]. Worsnopp et al. [6] introduced a finger exoskeleton for hand rehabilitation following stroke, to facilitate movement, especially pinch. Another

V. Petuya et al. (eds.), *New Advances in Mechanisms, Transmissions and Applications*, Mechanisms and Machine Science 17,
DOI: 10.1007/978-94-007-7485-8_15, © Springer Science+Business Media Dordrecht 2014

project is being developed by Ho et al. [7]: their exoskeleton hand is EMG-driven, again for rehabilitation, but working on all the fingers. All of these projects present a different number of DoFs and different structures, but in general they are developed with the objective of mimicking the main characteristics of the human hand. The current paper provides a general kinematic and dynamic model of a human hand, representing a mathematical tool to conceive and test new robotic hand-related devices.

2 Kinematic Model of the Human Hand

The kinematic model of the human hand here proposed is composed of 19 links corresponding to the bones and 24 DoFs modeled by joints. Two kinematic configurations are considered for the digits: the thumb is modeled as 3 links and 4 joints, while the fingers (index, middle, ring and little) are modeled as 4 links and 5 joints, see Figure 1. In the following, only the four fingers are analyzed, while the thumb is neglected. The direct kinematics, that permits to obtain the fingertip position and orientation according to the joint angles, is here solved. The model equations are calculated by means of Modified Denavit-Hartenberg (MDH) parameters, introduced by J. J. Craig [8].

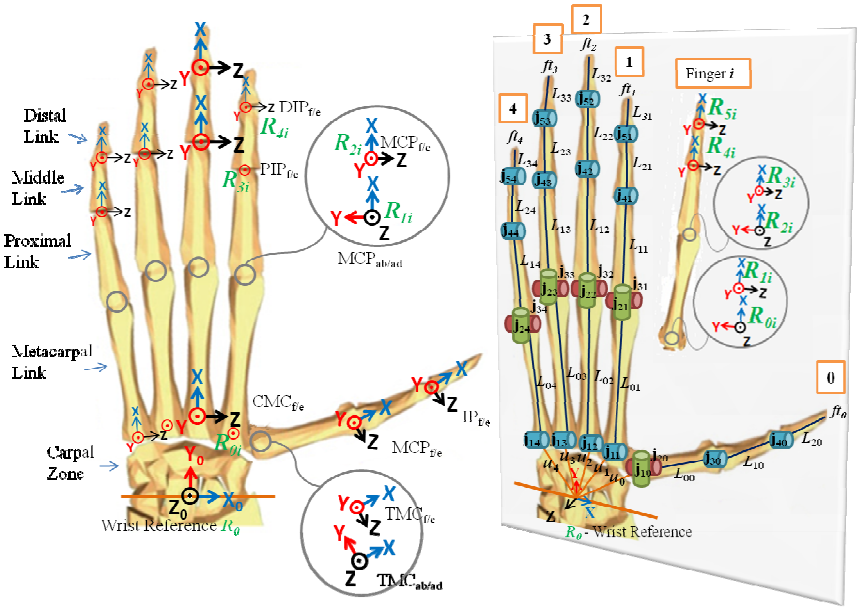

Fig. 1 Kinematic configuration of the human hand

The four bones of each finger correspond to the links of a serial kinematic chain, as represented in Figure 1. Each articulation for these four fingers

corresponds to the joints: CarpoMetaCarpal (CMC), MetaCarpoPhalangeal (MCP), Proximal InterPhalangeal (PIP), and Distal InterPhalangeal (DIP). The CMC joint represents the deformation of the palm, for instance when the hand is grasping a ball, while the MCP joint can be split into 2 DoFs, which carry out the adduction/abduction and flexion/extension movements respectively. All the other joints only allow flexion/extension movements. The digits are numbered from 0 to 4: digit 0 is the thumb and digits 1 to 4 range from the index to the little finger. The following table reports the MDH parameters for all the fingers.

Table 1 MDH parameters of the fingers

Joint	α_{i-1}	a_{i-1}	d_i	θ_i
j_{1i}	$\pi/2$	0	0	$\theta_{CMC_{f/e}}$
j_{2i}	$-\pi/2$	L_{01}	0	$\theta_{MCP_{ab/ad}}$
j_{3i}	$\pi/2$	0	0	$\theta_{MCP_{f/e}}$
j_{4i}	0	L_{11}	0	$\theta_{PIP_{f/e}}$
j_{5i}	0	L_{21}	0	$\theta_{DIP_{f/e}}$

Eq. (1) shows the direct kinematics from index (i=1) to the little finger (i=4):

$$\mathrm{Q_i} = {}^{0}_{0}\mathrm{T_i}\cdot {}^{0}_{6}\mathrm{T_i}(\theta_\mathrm{j}) = {}^{0}_{0}\mathrm{T_i}\cdot \prod_{\mathrm{j}=1}^{5} {}^{(\mathrm{j}-1)}_{\mathrm{j}}\mathrm{T_i}(\theta_\mathrm{j}) \cdot {}^{5}_{6}\mathrm{T}_{\mathrm{ft_i}} =$$

$$= {}^{0}_{0}\mathrm{T_i} \cdot {}^{0}_{1}\mathrm{T_i}(\theta_{\mathrm{CMC_{f/e}}}) \cdot {}^{1}_{2}\mathrm{T_i}(\theta_{\mathrm{MCP_{ab/ad}}}) \cdot {}^{2}_{3}\mathrm{T_i}(\theta_{\mathrm{MCP_{f/e}}}) \cdot {}^{3}_{4}\mathrm{T_i}(\theta_{\mathrm{PIP_{f/e}}}) \cdot {}^{4}_{5}\mathrm{T_i}(\theta_{\mathrm{DIP_{f/e}}}) \cdot {}^{5}_{6}\mathrm{T}_{\mathrm{ft_i}} \quad (1)$$

where:

- $\mathrm{Q_i}$ is a matrix containing position and orientation of the fingertip of each finger.
- ${}^{0}_{0}T_i$ represents a roto-translation matrix taking into account the fact that the fingers are slightly fanned out and allowing to pass from the initial base reference frame (R_0) to the alignment of the i-th finger first reference frame (R_{0i}).
- ${}^{0}_{6}T_i(\theta_j)$ is a matrix containing the geometrical transformation between the i-th finger first reference frame and the i-th fingertip (ft_i). The matrix is composed of the concatenation of the transformation matrices of each finger link.
- ${}^{(\mathrm{j}-1)}_{\mathrm{j}}\mathrm{T_i}(\theta_\mathrm{j})$ is a matrix containing the geometrical transformation between the (j-*1*)-th reference frame and the j-th reference frame of the i-th finger.
- ${}^{5}_{6}T_{ft_i}$ represents the position of the fingertip with respect to the distal (5th) reference frame.

j corresponds to each finger's joint $CMC_{f/e}$, $MCP_{ab/ad}$, $MCP_{f/e}$, $PIP_{f/e}$, $DIP_{f/e}$. ft_i stands for the fingertip of i-th finger.

3 Dynamics of a Single Finger

This section provides the dynamics equation system of a generic single finger, represented in Figure 2. The CMC DoF, that deals with the palm, and the MCP abduction/adduction one are neglected, since their range of movement is very low. For sake of brevity, in the following the i index is omitted, and $c\theta_j$ and $s\theta_j$ stand for cosine and sine of θ_j, respectively. The metacarpus is assumed as fixed, while only the finger phalanges are moving parts. Thus, R_2 is the base reference system, and all the equations are written with respect to R_2. The following equations can be recognized as applicable to any 3-R planar serial robot.

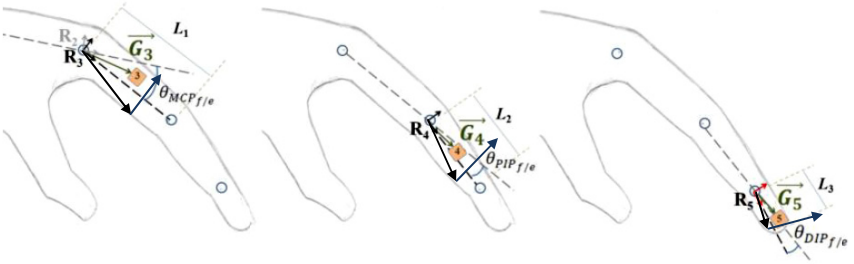

Fig. 2 Dynamic model of a finger

The dynamic model is determined using Euler–Lagrange equations. The kinetic energy is calculated starting from the position vectors of the center of mass of each phalanx with respect to the base reference frame R_2; in general, the position of the center of mass of the j-th phalanx with respect to the j reference frame is $\mathbf{G}_j = [b_{jx} \quad b_{jy} \quad 0]^T$, where j=3,4,5. The mass of the j-th phalanx is m_j and the respective moment of inertia with respect to the axis z is I_j. The following change of coordinates is introduced:

$$\psi_3 = \theta_{MCP_{f/e}}; \quad \psi_4 = \theta_{MCP_{f/e}} + \theta_{PIP_{f/e}}; \quad \psi_5 = \theta_{MCP_{f/e}} + \theta_{PIP_{f/e}} + \theta_{DIP_{f/e}} \quad (2)$$

The generic position vector of the center of mass with respect to the base reference frame R_2 is:

$$\mathbf{G}_j = [G_{jx} \quad G_{jy} \quad G_{jz}]^T = \sum_{q=3}^{j-1} \begin{bmatrix} L_{q-2} c\psi_q \\ L_{q-2} s\psi_q \\ 0 \end{bmatrix} + \begin{bmatrix} b_{jx} c\psi_j - b_{jy} s\psi_j \\ b_{jx} s\psi_j + b_{jy} c\psi_j \\ 0 \end{bmatrix} \quad (3)$$

The velocity of the generic center of mass is obtained:

$$\mathbf{v}_{G_j} = \sum_{q=3}^{j-1} \begin{bmatrix} -L_{q-2}\dot{\psi}_q s\psi_q \\ L_{q-2}\dot{\psi}_q c\psi_q \\ 0 \end{bmatrix} + \begin{bmatrix} -b_{jx}\dot{\psi}_j s\psi_j - b_{jy}\dot{\psi}_j c\psi_j \\ b_{jx}\dot{\psi}_j c\psi_j - b_{jy}\dot{\psi}_j s\psi_j \\ 0 \end{bmatrix} \tag{4}$$

The kinetic energy is thus expressed as:

$$T = \frac{1}{2}\sum_{j=3}^{5}\left(m_j v_{G_j}^2 + I_j \dot{\psi}_j^{\,2}\right) \tag{5}$$

The potential energy includes a gravitational term and an elastic one. Regarding the latter, the stiffness is considered as an average constant value k_j in this study, as a close approximation of the non-linear and anisotropic finger stiffness (i.e. it varies with the direction). k_3, k_4 and k_5 are the stiffness values for the MCP, DIP and PIP joints, respectively [9]. The potential energy is expressed as:

$$U = \sum_{j=3}^{5}\left(m_j g G_{jy} + \frac{1}{2}k_j\left(\psi_j - \psi_{j-1}\right)^2\right) \tag{6}$$

Moreover, a function of the generalized velocities, usually referred to as the Rayleigh dissipation function F, is introduced for the damping forces; it is expressed as:

$$F = \sum_{j=3}^{5}\left(\frac{1}{2}\beta_j\left(\dot{\psi}_j - \dot{\psi}_{j-1}\right)^2\right) \tag{7}$$

Where the damping constant β_j stands for the non-conservative contribution, caused by the muscles actuating the finger. Non-conservative forces contributed less than 15% to the total force response to static displacement. Muscle viscosity is dissipative and, hence, non-conservative, resulting in a force field with nonzero curl [9]. To be more precise, values β_3, β_4 and β_5 are the damping values for the MCP, DIP and PIP joints respectively. Considering the generalized coordinates ψ_j the Euler–Lagrange equations become:

$$\frac{d}{dt}\left(\frac{\partial(T-U)}{\partial\dot{\psi}_j}\right) - \frac{\partial(T-U)}{\partial\psi_j} + \frac{\partial F}{\partial\dot{\psi}_j} = \tau_j \tag{8}$$

Where j= 3, 4, 5. The τ_j terms contain the forces applied through the muscles in order to actuate the phalanges and the contact forces. According to the virtual work principle, the generalized force τ_j is:

$$\tau_j = \frac{\sum_{j=3}^{5}\delta W_j}{\delta\psi_j} \tag{9}$$

Where δW_j is the virtual work done by the force applied to the system. Then, it is:

$$\tau_j = \left(F_{jy}e_{jx} - F_{jx}e_{jy}\right) + \sum_{q=j+1}^{5} \begin{bmatrix} -L_{(j-2)}s\theta_j \\ L_{(j-2)}c\theta_j \\ 0 \end{bmatrix} \cdot \begin{bmatrix} F_{qx}c\psi_q - F_{qy}s\psi_q \\ F_{qx}s\psi_q + F_{qy}c\psi_q \\ 0 \end{bmatrix} + C_{mj} - C_{m(j+1)} \tag{10}$$

where the term C_{mj} refers to the torque produced by the muscles on the *j*-th joint, and $\mathbf{F}_j = [F_{jx} \quad F_{jy} \quad 0]^T$ is the contact force applied to the *j*-th phalanx at the point defined by the position vector $\mathbf{e}_j = [e_{jx} \quad e_{jy} \quad 0]^T$.

Calculating each element of the Euler–Lagrange equations, the dynamical system in Eq. (8) can be written in matricial form:

$$[A] \cdot [\ddot{\psi}_3 \quad \ddot{\psi}_4 \quad \ddot{\psi}_5]^T = [B] \tag{11}$$

where the 3x3 matrix [A] contains the coefficients of the accelerations, and the 3x1 vector [B] contains the remaining terms.

Eq. (11) allows the direct dynamics of the finger to be solved, where, given the torques exerted by the muscles on each phalange, the movement of the finger can be calculated. If, on the other side, an inverse dynamics problem is set, it is simple to rearrange Eq. (11) to obtain the trend of the unknown muscle torques from the phalanges motion laws.

4 Simulation

The current section deals with the implementation of the dynamics equations. Anthropometric data [10, 11] and proper numerical constants have been imposed, and a realistic circular grasping movement for a human finger is imposed.

In particular, the simulation shown here deals with an inverse dynamics case study: given the motion law of the system (i.e., the kinematic angles of the phalanges and their time derivatives), the torques exerted by the muscles on each phalanx are calculated. Figure 3 shows the imposed trend of each angle in time, starting from the straight position (angles=0°) and performing a flexion movement, then simulating a circular grasping operation. The angle proportions between the phalanges descend from physiological constraints [12, 13], as well as typical circular grasping proportions. Figure 4 shows the C_{m3}, C_{m4}, and C_{m5} torque values, required to perform this grasping operation. The maximum values of the contact forces used in the simulation were obtained from An et al. [14], which reports the maximum mid-phalangeal joint normal forces exerted by human fingers in a cylindrical power grasp, with values for the index finger of $\mathbf{F}_{max} = [42 \quad 22 \quad 62]^T$N for the proximal, middle and distal phalanx, respectively. Each column in the figure deals with a single simulation: case a) 100% F_{max}; case b) 50% F_{max}; and case c) 25% F_{max}. The a)-column graphs allow a comparison with

the data collected by Hasser [15]: this work states that the maximum torque capabilities of the human hand are $\mathbf{C}_{\mathrm{m_max}} = [4630 \quad 2280 \quad 775]^{\mathrm{T}}$Nmm for the proximal, middle and distal phalanx, respectively. The maximum torque values of the simulated C_{m4} and C_{m5} are very similar to the literature data, with a difference of 3.2% and 4% respectively. On the other side, the result for C_{m3} is quite different. This may be caused by the fact (not explicitly mentioned) that perhaps not all the three maximum forces can be exerted contemporarily.

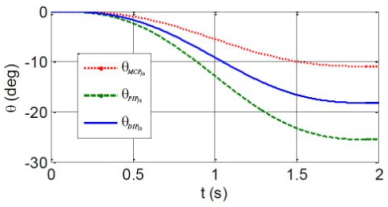

Fig. 3 Behavior of the joint angles in time

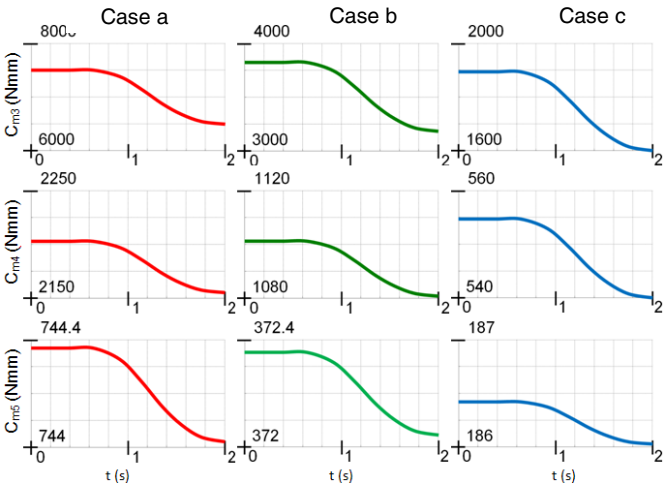

Fig. 4 Inverse dynamics case: behavior of the torques C_{mi} with respect to time

5 Conclusions

An exhaustive study of the human hand was performed, dealing with the kinematics of the human hand and showing the matrices with the MDH parameters and detailed equations to solve the kinematics of the hand. In addition, the dynamics of a single finger was analyzed and solved. A case study was proposed and a simulation was completed using the provided anthropometric data, in order to investigate the capabilities of the proposed analytical system.

The results of the current study can be exploited to conceive future hand devices. In fact, the study of the kinematics and the dynamics constitute a preliminary stage for the development of any structure similar to the human hand, for instance, in robotic or rehabilitation hands projects. Hence, the value of this analytical frame is twofold: to model the finger itself, for example to be used in a control scheme model of a human-machine interface, such as a hand exoskeleton or to model a finger-like architecture, such as a robotic hand.

References

1. Schoonejans, P., Stott, R., Didot, F., Allegra, A., Pensavalle, E., Heemskerk, C.: Eurobot: EVA-assistant robot for ISS, Moon and Mars. In: Proc. 8th ESA Workshop on Advanced Space Technologies for Robotics and Automation, Noordwijk (November 2004)
2. Lovchik, C.S., Diftler, M.A.: The robonaut hand: A dexterous robot hand for space. In: Proc. IEEE Int. Conf. Robotics and Automation (1999)
3. Jordan, N., Saleh, J., Newman, D.: The extravehicular mobility unit: A review of environment, requirements, and design changes in the US spacesuit. Acta Astronautica 59, 1135–1145 (2006)
4. Schabowsky, C.N., Godfrey, S.B., Holley, R.J., Lum, P.S.: Development and pilot testing of HEXORR: Hand EXOskeleton Rehabilitation Robot. Journal of Neuroengineering and Rehabilitation (2010)
5. http://www.nasa.gov/mission_pages/station/main/robo-glove.html
6. Worsnopp, T.T., Peshkin, M.A., Colgate, J.E., Kamper, D.G.: An Actuated Finger Exoskeleton for Hand Rehabilitation Following Stroke. In: Proceedings of the 2007 IEEE 10th International Conference on Rehabilitation Robotics, Noordwijk, The Netherlands, June 12-15 (2007)
7. Ho, N.S.K., Tong, K.Y., Hu, X.L., Fung, K.L., Wei, X.J., Rong, W., Susanto, E.A.: An EMG-driven Exoskeleton Hand Robotic Training Device on Chronic Stroke Subjects. In: 2011 IEEE International Conference on Rehabilitation Robotics Rehab Week Zurich, ETH Zurich Science City, Switzerland, June 29-July 1 (January 2011)
8. Craig, J.J.: Introduction to Robotics, Mechanics and Control, 3rd edn., pp. 67–76. Pearson Education International (1986)
9. Milner, T.E., Franklin, D.W.: Characterization of multijoint finger stiffness: dependence on finger posture and force direction. IEEE Transactions on Biomedical Engineering 45(11), 1363–1375 (1998)
10. Habib, S.R., Kamal, N.N.: Stature estimation from hand and phalanges lengths of Egyptians. Journal of Forensic and Legal Medicine 17(3), 156–160 (2010)
11. Jasuja, O.P., Singh, G.: Estimation of stature from hand and phalange length. Journal of Indian Academy of Forensic Medicine 26(3) (2004)
12. Rijpkema, H., Girard, M.: Computer animation of knowledge-based human grasping. In: Proceedings of Siggraph, pp. 339–348 (1991)
13. Cobos, S., Ferre, M., Sanchez, M., Ortego, J.: Constraints for Realistic Hand Manipulation. In: The 10th Annual International Workshop on Presence, PRESENCE 2007, Barcelona, Spain, October 25-27 (2007)
14. An, K.N., Askew, L., Chao, E.Y.: Biomechanics and Functional Assessment of Upper Extremities. In: Karwowski, W. (ed.) Trends in Ergonomics/Human Factors III, pp. 573–580 (1986)
15. Hasser, C.J.: Force-Reflecting Anthropomorphic Hand Masters. Armstrong Lab Wright-Patterson AFB Oh Crew Systems Directorate, 37 p. (July 1995)